

MYL9 promotes squamous cervical cancer migration and invasion by enhancing aerobic glycolysis

Journal of International Medical Research

2023, Vol. 51(11) 1–9

© The Author(s) 2023

Article reuse guidelines:

sagepub.com/journals-permissions

DOI: 10.1177/03000605231208582

journals.sagepub.com/home/imr



Bin Wen^{1,2} , Limei Luo^{3,4}, Zhaoyang Zeng⁴
and Xiping Luo^{1,2} 

Abstract

Objective: This study explored the mechanism of squamous cervical cancer (SCC) progression.

Methods: Reverse transcription-quantitative polymerase chain reaction and western blotting were used to evaluate the expression of myosin light chain 9 (MYL9) in SCC tissues and cell lines. Furthermore, Transwell and Boyden assays were used to assess the function of MYL9 in SCC progression. In addition, the levels of lactate and aerobic glycolysis were used to explore the detailed mechanism of MYL9 in SCC.

Results: The mRNA and protein levels of MYL9 were elevated in SCC tissues, and MYL9 knock-down inhibited the migration and invasion of SCC cell lines. A mechanistic study demonstrated that MYL9 promotes SCC migration and invasion by enhancing aerobic glycolysis and increasing the activity of the Janus kinase 2 (JAK2)/signal transducer and activator of transcription 3 (STAT3) pathway.

Conclusions: MYL9 was upregulated in SCC, and it enhanced JAK2/STAT3 pathway activity and promoted metastasis and glycolysis in SCC.

Keywords

Myosin light chain 9, squamous cervical cancer, aerobic glycolysis, migration, invasion, Janus kinase 2, signal transducer, activator of transcription

Date received: 11 January 2023; accepted: 2 October 2023

⁴Department of Gynecology, Integrated Hospital of Traditional Chinese Medicine, Southern Medical University, Guangzhou, P.R. China

Corresponding author:

Xiping Luo, Department of Gynecology, Guangdong Women and Children Hospital, No 521, Xing Nan Da Dao, Panyu District, Guangzhou 511442, Guangdong, P.R. China.

Email: luoxiping333@126.com

¹The First Clinical College of Jinan University, Guangzhou, Guangdong, P.R. China

²Department of Gynecology, Guangdong Women and Children Hospital, Guangzhou, P. R. China

³The Second Clinical College, Guangzhou University of Chinese Medicine, Guangdong, P.R. China



Creative Commons Non Commercial CC BY-NC: This article is distributed under the terms of the Creative

Commons Attribution-NonCommercial 4.0 License (<https://creativecommons.org/licenses/by-nc/4.0/>) which permits non-commercial use, reproduction and distribution of the work without further permission provided the original work is attributed as specified on the SAGE and Open Access pages (<https://us.sagepub.com/en-us/nam/open-access-at-sage>).

Introduction

Cervical cancer is the most common cancer in developing countries, and squamous cervical cancer (SCC) is the most common cancer globally.¹⁻³ Although persistent high-risk human papillomavirus (HPV) infection is the main risk factor for SCC,⁴ the detailed molecular mechanisms of migration/invasion in SCC are unclear. Thus, it is essential to study the detailed mechanisms driving the progression of SCC, which could facilitate the development of effective targeted therapeutic methods and decrease the morbidity and mortality of SCC.

Myosin light chain 9 (*MYL9*) encodes the regulatory light chain of myosin II (the most studied member of the myosin superfamily) and plays a crucial role in tumor progression and metastases.⁵⁻¹¹ Accumulating evidence indicates that *MYL9* is differentially expressed in various human tissues. Total *MYL9* expression is lower in colon, gastric, bladder, non-small cell lung, and prostate cancers^{10,12-15} than in the corresponding normal tissues. Conversely, *MYL9* is upregulated in ovarian cancer,¹⁶ esophageal squamous cell carcinoma,⁵ and glioblastoma,⁸ and its overexpression is correlated with poor clinical outcomes. A previous study demonstrated that *MYL9* induced aerobic glycolysis in endometrial fibroblasts.¹⁷ However, to our knowledge, the detailed mechanism, expression, and function of *MYL9* in SCC have not yet been reported.

When tumor cells have good oxygen availability, they utilize glycogen and undergo aerobic glycolysis (Warburg effect), thereby generating high levels of lactate. Glycolysis plays an important role in the occurrence and development of tumors, but the detailed molecular mechanisms remain to be clarified. Glucose transporter (GLUT1), a transmembrane protein, is responsible for the uptake of glucose into the cells of many tissues through

facilitative diffusion.¹⁸ Hexokinase II (HK2) is a predominant isoform in insulin-sensitive tissues, and it is also upregulated in many types of tumors associated with enhanced aerobic glycolysis.¹⁹ Lactate dehydrogenase A (LDHA) is a glycolysis enzyme that converts pyruvate to lactate.²⁰

Our research demonstrated that *MYL9* is upregulated in SCC, and it promotes migration and invasion by accelerating glycolysis. In addition, *MYL9* activates the Janus kinase 2 (JAK2)/signal transducer and activator of transcription 3 (STAT3) signaling pathway, thereby promoting tumor progression in SCC.

Materials and methods

Cells and tissues

Human SCC cell lines (Siha, contains integrated copies of HPV-16; Caski, contains integrated copies of HPV-16 and HPV-18) were obtained from the Cell Resource Center, Shanghai Institute of Life Sciences, Chinese Academy of Sciences (Shanghai, China). Both cell lines were cultured in high-glucose Dulbecco's Modified Eagle's Medium (Thermo Fisher Scientific, Waltham, MA, USA) supplemented with 10% fetal bovine serum (FBS; Cytiva, Marlborough, MA, USA), and cells were cultured at 37°C in an atmosphere of 5% CO₂. In addition, 36 pairs of matched SCC and healthy tissues were acquired from patients who underwent surgery at the Integrated Hospital of Traditional Chinese Medicine, Southern Medical University. Written informed consent was obtained from all patients before surgery, and this research was approved by the hospital's ethics committee (No.: NFZXYEC-201906sb-K1). All procedures performed in this study followed with the ethical standards of the institutional research committee and the 1964 Declaration of Helsinki

and its later amendments or comparable ethical standards.

Reverse transcription-quantitative polymerase chain reaction (RT-qPCR)

The mRNA sequences of clinical tissues or SCC cells were detected and quantified using RT-qPCR to better explore *MYL9* gene expression. Total RNA was extracted from SCC tissues or cell lines using TRIzol (Takara Bio, Inc., Shiga, Japan). Complementary DNA (cDNA) was synthesized from 1 μ g of total RNA using SuperScript III RT (Thermo Fisher Scientific). The PCR mix contained 1 μ L of cDNA, 1 \times SYBR Green (Toyobo, Osaka, Japan), and specific primers. The primers were synthesized by IGE Co., Ltd (Guangzhou, China). The experiments were conducted more than three times using LightCycler 480 II (Roche, Basel, Switzerland). Glyceraldehyde 3-phosphate dehydrogenase (*GAPDH*) mRNA expression was detected as the internal control. The expression in each matched fresh peritumoral tissue sample was set as the control (the expression of *MYL9* in all peritumoral tissues was set as 1), and the relative expression was determined by the $2^{-\Delta\Delta C_t}$ method.²¹ The thermocycling conditions¹⁷ were 95°C for 10 minutes to activate DNA polymerase, followed by 45 cycles of 95°C for 15 s, 60°C for 15 s, and 72°C for 10 s. The specificity of amplification products was confirmed by melting curve analysis. Independent experiments were performed in triplicate. The primer sequences used in the polymerase chain reaction (PCR)¹⁶ were as follows: *MYL9* forward, 5'-GCCACATCCAATGTCTTCGC-3'; *MYL9* reverse, 5'-GCGTTGCGAATCACATCCTC-3'; *GAPDH* forward, 5'-CCATCTTCCAGGAGCGAGAT-3'; and *GAPDH* reverse, 5'-TGCTGATGATCTTAGGCTG-3'.

Transfection

siRNA targeting *MYL9* (siMYL9) was designed by Guangzhou Ribobio Co., Ltd. (Guangzhou, China). The specific sequence of siMYL9 was 5'-GCAACATCGTCTTC AAGAA-3'. SiRNA (concentration: 50 nM, 10 μ L) was transfected into Siha and Caski cells using Lipofectamine® 2000 (Thermo Fisher Scientific) according to the manufacturer's protocol.

Transwell and Boyden assays

SCC cell migration and invasion assays were performed using Transwell chambers (8 μ m, 24-well insert; Corning Inc., Corning, NY, USA). For the Transwell assay, cells (1×10^5) in serum-free medium were added to the upper chamber, and medium containing 20% FBS was added to the lower chamber. Cells were incubated for 12 hours at room temperature. For the Boyden assay, diluted Matrigel (BD Biosciences, Franklin Lakes, NJ, USA) was used to pre-coat the insert membrane. Cells (1×10^5) were cultured for 36 hours under the same conditions. Finally, the cells that migrated to or invaded the lower chambers were fixed with methanol, stained with Giemsa or crystal violet, and counted in six random fields under a microscope (BDS200, Olympus, Tokyo, Japan).

Lactate production assay

A lactate assay kit (Abcam, Cambridge, UK) was used to detect lactate production colorimetrically per the manufacturer's protocols. siRNA-transfected SCC cells were seeded into a 96-well cell culture plate and incubated overnight at 37°C. The cells were subsequently starved for 12 hours, and the supernatant was obtained and used to detect lactate levels using a microplate reader (Biotek, Winooski, VT, USA) at 450 nm.

Western blotting

Flasks containing SCC cells were washed three times with ice-cold phosphate-buffered saline, and total protein was harvested using RIPA lysis buffer (Beyotime Institute of Biotechnology, Jiangsu, China) containing phenylmethanesulfonyl fluoride (Bio-Rad Laboratories, Inc., Hercules, CA, USA) and phosphatase inhibitors (Bio-Rad Laboratories) at a ratio of 100:1:1. A bicinchoninic acid protein assay kit (Beyotime Institute of Biotechnology) was used to determine the protein concentrations. Proteins (30 µg) were separated by sodium dodecyl sulfate-polyacrylamide gel electrophoresis on 10% gels and transferred to a polyvinylidene fluoride membrane (Beyotime Institute of Biotechnology). The membranes were blocked with 5% bovine serum albumin in TBS containing Tween-20 (TBST) for 1 hour at 37°C and incubated with primary antibodies against *MYL9* (mouse, 60233-1-Ig, Proteintech, Rosemont, IL, USA), GLUT1 (rabbit, 21829-1-AP, Proteintech), HK2 (mouse, 66974-1-Ig, Proteintech), LDHA (rabbit, 19987-1-AP, Proteintech), β-tubulin (mouse, Proteintech), and GAPDH (mouse, CW0100M, CWBIO, Beijing, China) overnight at 4°C. Following three washes with TBST, the membrane was incubated with horseradish peroxidase-conjugated goat anti-rabbit or anti-mouse IgG antibody at 37°C for 1 hour. The membranes were visualized using an electrochemiluminescence chromogenic kit (Beyotime Institute of Biotechnology) in a dark room, and images were captured with a ChemiDoc™ Molecular Imager (Bio-Rad Laboratories). The experiments were repeated at least three times.

Statistical analysis

All experiments were performed in sets of three or more, and all data were presented as the mean ± standard deviation.

The differences between the two groups were analyzed using Student's *t*-test, and graphs were plotted using GraphPad Prism 7 (GraphPad Software, Inc.,

Table 1. The detailed information of 36 patients with SCC.

Patient	Age (years)	Stage	<i>MYL9</i> mRNA expression
Patient 1	48	IB3	3.1380 ± 0.9234
Patient 2	52	IIA1	5.1940 ± 1.1850
Patient 3	43	IB2	8.3520 ± 1.0540
Patient 4	47	IIA1	0.5990 ± 0.3972
Patient 5	45	IB1	14.510 ± 1.0660
Patient 6	45	IB3	0.3807 ± 0.0374
Patient 7	51	IIA2	19.180 ± 0.4058
Patient 8	46	IB2	8.2830 ± 0.8320
Patient 9	57	IIA1	0.2337 ± 0.0900
Patient 10	51	IIA1	6.1160 ± 0.2013
Patient 11	50	IB2	5.8330 ± 0.1338
Patient 12	49	IB3	3.3220 ± 0.1209
Patient 13	52	IB3	5.6870 ± 0.3392
Patient 14	50	IIA1	4.5690 ± 0.3886
Patient 15	46	IB3	8.6820 ± 0.2989
Patient 16	43	IB1	7.3430 ± 0.4162
Patient 17	47	IIA1	4.9330 ± 0.6782
Patient 18	54	IB2	6.7750 ± 0.9384
Patient 19	56	IIA2	10.080 ± 0.9134
Patient 20	55	IB3	3.6370 ± 0.3634
Patient 21	39	IB3	6.5810 ± 0.3866
Patient 22	32	IB1	2.6640 ± 0.4247
Patient 23	28	IB2	5.3360 ± 0.2440
Patient 24	51	IIA1	0.1560 ± 0.0243
Patient 25	43	IB2	8.6230 ± 0.2416
Patient 26	42	IB3	6.4760 ± 0.3943
Patient 27	48	IB3	3.9330 ± 0.4258
Patient 28	55	IIA1	7.3530 ± 0.3752
Patient 29	49	IB1	4.2390 ± 0.2203
Patient 30	42	IB2	0.2448 ± 0.0638
Patient 31	48	IB3	6.5170 ± 0.4408
Patient 32	57	IIA1	5.4730 ± 0.3377
Patient 33	59	IB3	7.3320 ± 0.2346
Patient 34	52	IB2	5.5320 ± 0.3985
Patient 35	51	IB3	4.9820 ± 0.2929
Patient 36	53	IIA2	5.6160 ± 0.3797

SCC, squamous cervical carcinoma.

San Diego, CA, USA). $P < 0.05$ was considered statistically significant.

Results

MYL9 is upregulated in SCC

Using 36 pairs of SCC and peritumoral tissues (Table 1), we observed a significant difference in the mRNA expression of *MYL9* between tumor and healthy tissue ($P < 0.0001$, Figure 1a, b). Additionally, *MYL9* protein was highly expressed in SCC cells (Figure 1c).

MYL9 knockdown suppresses in vitro SCC cell migration and invasion

We performed Transwell and Boyden assays to detect the role of *MYL9* in SCC. Our results indicated that SCC cell

migration and invasion were significantly suppressed by *MYL9* knockdown (Figure 2).

MYL9 promotes JAK2/STAT3 pathway activity and SCC migration and invasion by enhancing aerobic glycolysis

Owing to the close correlation between the progression of cancer cells and aerobic glycolysis, lactate levels were determined, and western blotting was performed. Interestingly, our results demonstrated that lactate levels were lower in the siMYL9 group (Figure 3a), and GLUT1, HK2, and LDHA protein expression was significantly inhibited after *MYL9* knockdown (Figure 3b). To further explore the mechanism of *MYL9* in aerobic glycolysis in SCC, western blotting was performed, and the phosphorylation of JAK2 and STAT3 was significantly reduced in the siMYL9 group (Figure 3c).

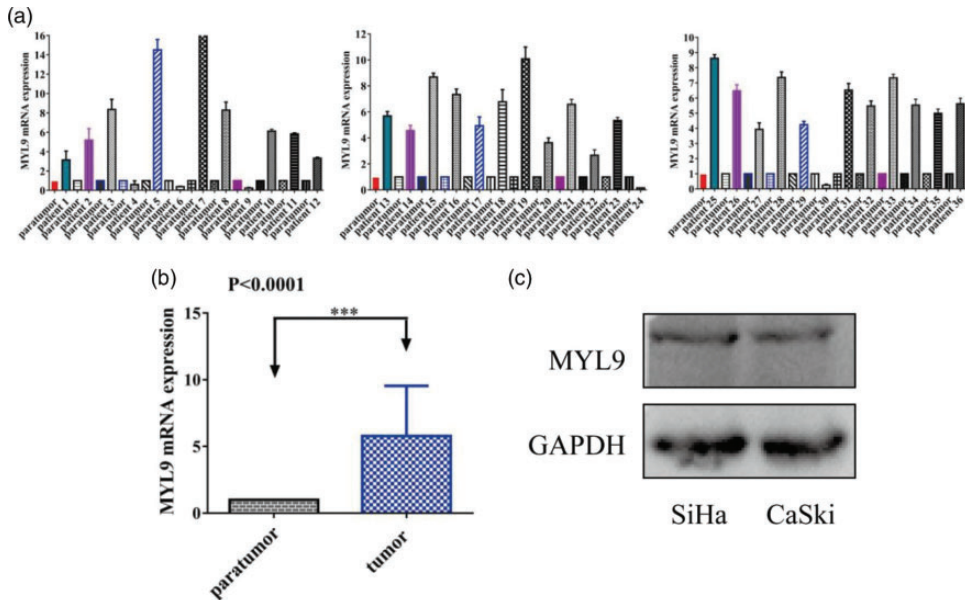


Figure 1. *MYL9* mRNA and protein expression in SCC tissues and cell lines. (a, b) Reverse transcription-quantitative polymerase chain reaction revealed higher *MYL9* mRNA expression in SCC tissues than in peritumoral tissues and (c) Western blotting illustrated that *MYL9* protein was expressed in SCC cells. *MYL9*, myosin light chain 9; SCC, squamous cervical cancer.

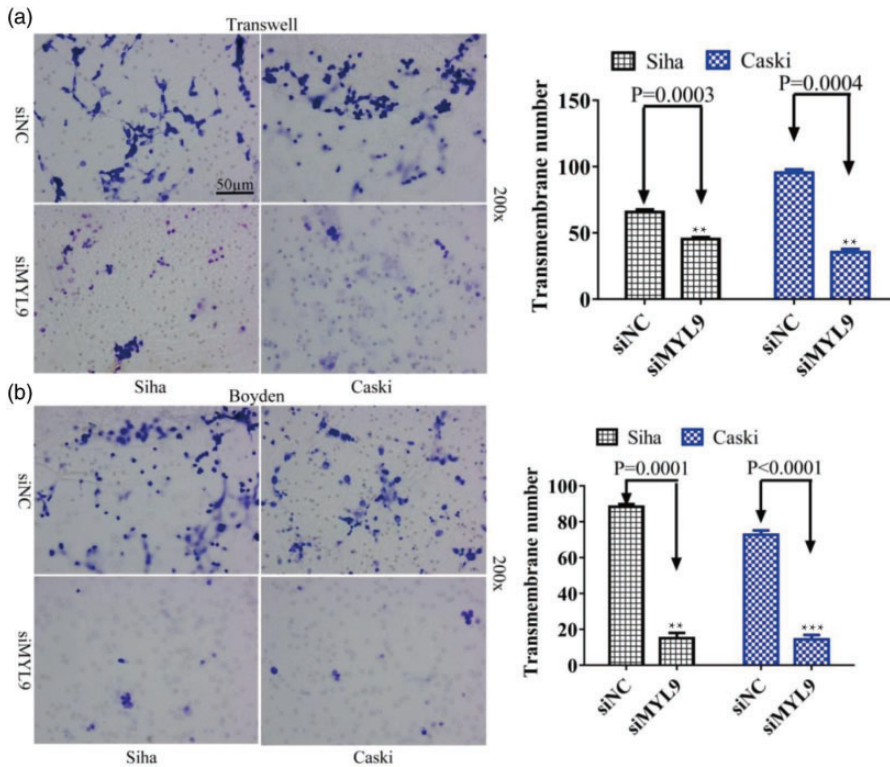


Figure 2. Transwell and Boyden assays demonstrated that *MYL9* knockdown suppresses SCC cell migration and invasion. (a) Knockdown of *MYL9* reduced the migration of SCC cells in the Transwell assay and (b) Knockdown of *MYL9* reduced cell invasion in SCC cells in the Boyden assay (magnification, $\times 200$; scale bar = $50\ \mu\text{m}$). *MYL9*, myosin light chain 9; SCC, squamous cervical cancer.

Thus, these findings indicated that *MYL9* induces JAK2/STAT3 pathway activity and promotes SCC migration and invasion by enhancing aerobic glycolysis.

Discussion

Recent studies illustrated that *MYL9* is weakly expressed in non-small cell lung, gastric, bladder, colon, and prostate cancers.^{10,12–15} However, other reports illustrated that *MYL9* is highly expressed in ovarian cancer, esophageal squamous cell carcinoma, and glioblastoma.^{5,8,16} To our knowledge, our study is the first to validate that *MYL9* is highly expressed in SCC

compared with its expression in peritumoral tissues, and *MYL9* protein expression was also high in SCC cell lines, thus indicating *MYL9* upregulation in SCC. However, additional studies are required to demonstrate its exact role in cancer.

Previous reports illustrated that *MYL9* participates in many physiological and pathological functions including cell adhesion, polarity, and motility, and it plays a crucial role in some human cancers.^{5,8,12–16} Previous studies also reported that *MYL9* plays a role in tumor suppression in gastric and colon cancers.^{10,12} On the contrary, other studies indicated that *MYL9* has an oncogenic role in melanoma, glioblastoma, and breast cancer.^{8,9,11}

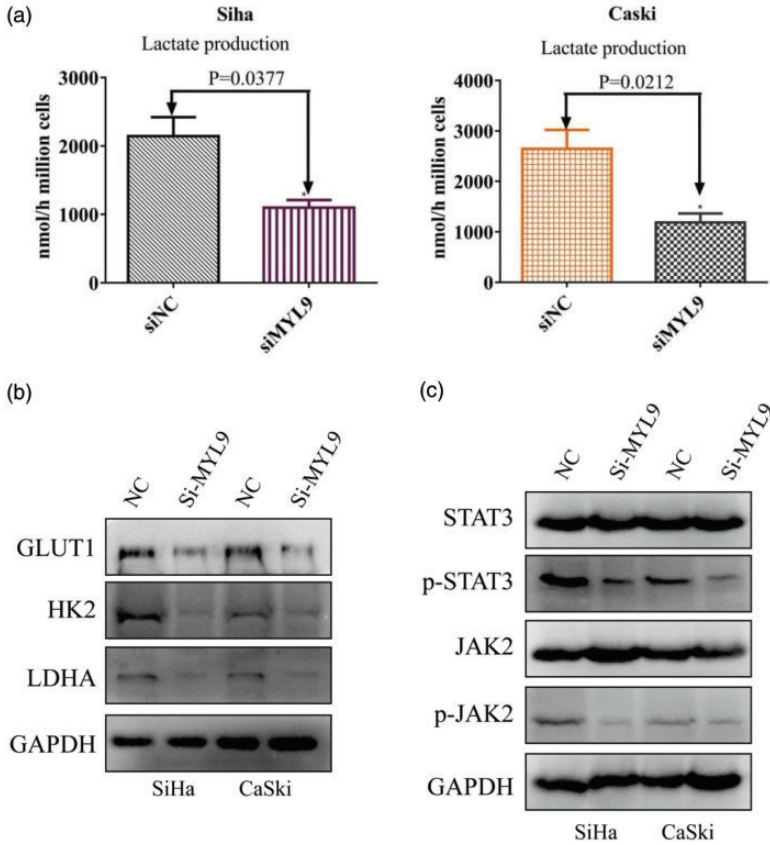


Figure 3. *MYL9* promoted the progression of SCC by enhancing aerobic glycolysis. (a) *MYL9* knockdown decreased the Lactate production of SCC. (b) *MYL9* knockdown inhibited the expression of GLUT1, HK2, and LDHA and (c) *MYL9* knockdown inactivated the JAK2/STAT3 pathway. *MYL9*, myosin light chain 9; SCC, squamous cervical cancer; GLUT1, glucose transporter 1; HK2, hexokinase II; LDHA, lactate dehydrogenase A.

GLUT1, *HK2*, and *LDHA* are key factors of aerobic glycolysis, and they play important roles in metabolic reprogramming and cancer progression.^{22–26} In this study, our results revealed that lactate levels were reduced in the *MYL9* knockdown group compared with that in the control group, and *GLUT1*, *HK2*, and *LDHA* expression in SCC cells was decreased after the *MYL9* gene was suppressed. *MYL9* promoted SCC cell migration and invasion *in vitro* by enhancing aerobic glycolysis. The JAK2/STAT3 signaling pathway has been reported to produce a marked effect on all

types of tumors.^{27–31} However, one limitation of the present study was that normal epithelial cells were not used as a control. Future studies are warranted to further demonstrate the detailed role of *MYL9* *in vivo*.

Collectively, our results revealed that *MYL9* was upregulated in SCC tissues compared with that in peritumoral samples, and *MYL9* knockdown inhibited the migration and invasion of SCC cells by regulating aerobic glycolysis and its downstream factors (including *GLUT1*, *HK2*, and *LDHA*) via the JAK2/STAT3 pathway. Thus, *MYL9* serves

as a metastasis-related gene in SCC, and it is a potential biomarker for targeted treatment.

Data availability statement

The datasets generated/analyzed during the present study are available.


Declaration of conflicting interest

The authors declare no conflicts of interest.

Funding

The present study was supported by the President funds of the Integrated Hospital of Traditional Chinese Medicine, Southern Medical University (No. 1201902001).

ORCID iDs

Bin Wen  <https://orcid.org/0000-0003-4731-6208>

Xiping Luo  <https://orcid.org/0000-0003-4303-3622>

References

- Nersesyan A, Muradyan R, Kundi M, et al. Smoking causes induction of micronuclei and other nuclear anomalies in cervical cells. *Int J Hyg Environ Health* 2020; 226: 113492. doi: 10.1016/j.ijheh.2020.113492.
- Lopez N, Gil-de-Miguel A, Pascual-Garcia R, et al. Reduction in the burden of hospital admissions due to cervical disease from 2003-2014 in Spain. *Hum Vaccin Immunother* 2018; 14: 917–923. doi: 10.1080/21645515.2017.1412897.
- Hull R, Mbele M, Makhafola T, et al. Cervical cancer in low and middle-income countries. *Oncol Lett* 2020; 20: 2058–2074. doi: 10.3892/ol.2020.11754.
- Ginsburg O and Horton R. A Lancet Commission on women and cancer. *Lancet* 2020; 396: 11–13. doi: 10.1016/S0140-6736(20)31479-3.
- Wang JH, Zhang L, Huang ST, et al. Expression and prognostic significance of MYL9 in esophageal squamous cell carcinoma. *PLoS One* 2017; 12: E175280. doi: 10.1371/journal.pone.0175280.
- Zhu K, Wang Y, Liu L, et al. Long non-coding RNA MBNL1-AS1 regulates proliferation, migration, and invasion of cancer stem cells in colon cancer by interacting with MYL9 via sponging microRNA-412-3p. *Clin Res Hepatol Gastroenterol* 2020; 44: 101–114. doi: 10.1016/j.clinre.2019.05.001.
- Zhao B, Baloch Z, Ma Y, et al. Identification of Potential Key Genes and Pathways in Early-Onset Colorectal Cancer Through Bioinformatics Analysis. *Cancer Control* 2019; 26: 1073274819831260. doi: 10.1177/1073274819831260.
- Kruthika BS, Sugur H, Nandaki K, et al. Expression pattern and prognostic significance of myosin light chain 9 (MYL9): a novel biomarker in glioblastoma. *J Clin Pathol* 2019; 72: 677–681. doi: 10.1136/jclinpath-2019-205834.
- Kim JS, Kim B, Lee HK, et al. Characterization of morphological changes of B16 melanoma cells under natural killer cell attack. *Int Immunopharmacol* 2019; 67: 366–371. doi: 10.1016/j.intimp.2018.12.037.
- Gu W, Ren JH, Zheng X, et al. Comprehensive analysis of expression profiles of long non-coding RNAs with associated ceRNA network involved in gastric cancer progression. *Mol Med Rep* 2019; 20: 2209–2218. doi: 10.3892/mmr.2019.10478.
- He H, Wang D, Yao H, et al. Transcriptional factors p300 and MRTF-A synergistically enhance the expression of migration-related genes in MCF-7 breast cancer cells. *Biochem Biophys Res Commun* 2015; 467: 813–820. doi: 10.1016/j.bbrc.2015.10.060.
- Yan Z, Li J, Xiong Y, et al. Identification of candidate colon cancer biomarkers by applying a random forest approach on microarray data. *Oncol Rep* 2012; 28: 1036–1042. doi: 10.3892/or.2012.1891.
- Lu Y, Liu P, Wen W, et al. Cross-species comparison of orthologous gene expression in human bladder cancer and carcinogen-induced rodent models. *Am J Transl Res* 2010; 3: 8–27.
- Tan X and Chen M. MYLK and MYL9 expression in non-small cell lung cancer identified by bioinformatics analysis of

- public expression data. *Tumour Biol* 2014; 35: 12189–12200. doi: 10.1007/s13277-014-2527-3.
15. Huang YQ, Han ZD, Liang YX, et al. Decreased expression of myosin light chain MYL9 in stroma predicts malignant progression and poor biochemical recurrence-free survival in prostate cancer. *Med Oncol* 2014; 31: 820. doi: 10.1007/s12032-013-0820-4.
 16. Deng Y, Liu L, Feng W, et al. High Expression of MYL9 Indicates Poor Clinical Prognosis of Epithelial Ovarian Cancer. *Recent Pat Anticancer Drug Discov* 2021; 16: 533–539. doi: 10.2174/1574891X16666210706153740.
 17. Afzal J, Du W, Novin A, et al. Paracrine HB-EGF signaling reduce enhanced contractile and energetic state of activated decidual fibroblasts by rebalancing SRF-MRTF-TCF transcriptional axis. *Front Cell Dev Biol* 2022; 10: 927631. doi: 10.3389/fcell.2022.927631.
 18. Zhang Z, Li X, Yang F, et al. DHHC9-mediated GLUT1 S-palmitoylation promotes glioblastoma glycolysis and tumorigenesis. *Nat Commun* 2021; 12: 5872. doi: 10.1038/s41467-021-26180-4.
 19. Tan VP and Miyamoto S. HK2/hexokinase-II integrates glycolysis and autophagy to confer cellular protection. *Autophagy* 2015; 11: 963–964. doi: 10.1080/15548627.2015.1042195.
 20. Xu K, Yin N, Peng M, et al. Glycolysis fuels phosphoinositide 3-kinase signaling to bolster T cell immunity. *Science* 2021; 371: 405–410. doi: 10.1126/science.abb2683.
 21. Livak KJ and Schmittgen TD. Analysis of relative gene expression data using real-time quantitative PCR and the 2⁻(Delta Delta C(T)) Method. *Methods* 2001; 25: 402–408. doi: 10.1006/meth.2001.1262.
 22. Fan Y, Hu D, Li D, et al. UCHL3 promotes aerobic glycolysis of pancreatic cancer through upregulating LDHA expression. *Clin Transl Oncol* 2021; 23: 1637–1645. doi: 10.1007/s12094-021-02565-1.
 23. Yang D, Chang S, Li F, et al. M⁶ A transferase KIAA1429-stabilized LINC00958 accelerates gastric cancer aerobic glycolysis through targeting GLUT1. *IUBMB Life* 2021; 73: 1325–1333. doi: 10.1002/iub.2545.
 24. Liu H, Zhang Q, Song Y, et al. Long non-coding RNA SLC2A1-AS1 induced by GLI3 promotes aerobic glycolysis and progression in esophageal squamous cell carcinoma by sponging miR-378a-3p to enhance Glut1 expression. *J Exp Clin Cancer Res* 2021; 40: 287. doi: 10.1186/s13046-021-02081-8.
 25. Lin C, Chen H, Han R, et al. Hexokinases II-mediated glycolysis governs susceptibility to crizotinib in ALK-positive non-small cell lung cancer. *Thorac Cancer* 2021; 12: 3184–3193. doi: 10.1111/1759-7714.14184.
 26. Jiang X, Guo S, Wang S, et al. EIF4A3-Induced circARHGAP29 Promotes Aerobic Glycolysis in Docetaxel-Resistant Prostate Cancer through IGF2BP2/c-Myc/LDHA Signaling. *Cancer Res* 2022; 82: 831–845. doi: 10.1158/0008-5472.CAN-21-2988.
 27. Liang Q, Gong M, Zou JH, et al. A phosphoglycerate mutase 1 allosteric inhibitor overcomes drug resistance to EGFR-targeted therapy via disrupting IL-6/JAK2/STAT3 signaling pathway in lung adenocarcinoma. *Drug Resist Updat* 2023; 68: 100957. doi: 10.1016/j.drug.2023.100957.
 28. Jin Y, Kang Y, Wang M, et al. Targeting polarized phenotype of microglia via IL6/JAK2/STAT3 signaling to reduce NSCLC brain metastasis. *Signal Transduct Target Ther* 2022; 7: 52. doi: 10.1038/s41392-022-00872-9.
 29. Kim MS, Lee HS, Kim YJ, et al. MEST induces Twist-1-mediated EMT through STAT3 activation in breast cancers. *Cell Death Differ* 2019; 26: 2594–2606. doi: 10.1038/s41418-019-0322-9.
 30. Reusswig F, Fazel MN, Brechtenkamp M, et al. Efficiently Restored Thrombopoietin Production by Ashwell-Morell Receptor and IL-6R Induced Janus Kinase 2/Signal Transducer and Activator of Transcription Signaling Early After Partial Hepatectomy. *Hepatology* 2021; 74: 411–427. doi: 10.1002/hep.31698.
 31. Sawashita Y, Hirata N, Yoshikawa Y, et al. Remote ischemic preconditioning reduces myocardial ischemia-reperfusion injury through unacylated ghrelin-induced activation of the JAK/STAT pathway. *Basic Res Cardiol* 2020; 115: 50. doi: 10.1007/s00395-020-0809-z.